Passive Cooling of Permafrost by Air Convection

1 Introduction

The preservation of the permafrost is often imperative to protect such structures as roads, railways, and runway embankments. Man-made structures generally alter the surface energy balance in a manner that causes an overall warming trend. Goering (2000) investigated passive cooling within an embankment constructed of unconventional and highly porous materials as means of preserving permafrost. Unstable density stratifications within the porous embankment led to the development of convective cells during the cold winter months. The convective cells enhanced energy transfer out of the earth structure, resulting in a deeper penetration of cold air within the embankment, which in-turn promoted preservation of the foundation permafrost layer.

Goering (2000) used a finite element program to numerically simulate the heat and air transfer that occurred in a full-scale field test (Goering and Kumar, 1996 and Goering, 1998). Goering (2000) focused on the air pressure boundary condition for the side-slope of the embankment and gave consideration to: (a) an open boundary which allowed for infiltration of ambient air; and b) a closed boundary which allowed for internal convection and no interaction with the atmosphere. The closed boundary represents, for example, high moisture content topsoil covering the porous embankment or snow cover during the winter months.

2 Feature Highlights

GeoStudio feature highlights include:

- Integration between SEEP/W, AIR/W and TEMP/W
- Numerical simulation of convective air cells within a porous material
- Alteration of the conduction-only isotherms caused by heat advection with air transfer

3 Numerical Model

Figure 1 presents the finite element domain used to represent the porous roadway embankment and underlying foundational soil. The symmetrical nature of the problem allowed only half of the domain to be simulated. The embankment roadway is 6 m wide, 2.5 m in height, and has 2:1 side-slopes. The mesh density was increased within the embankment and below the interface with the foundation, but decreased (i.e. element size increased) along the outside edges of the lowest region.

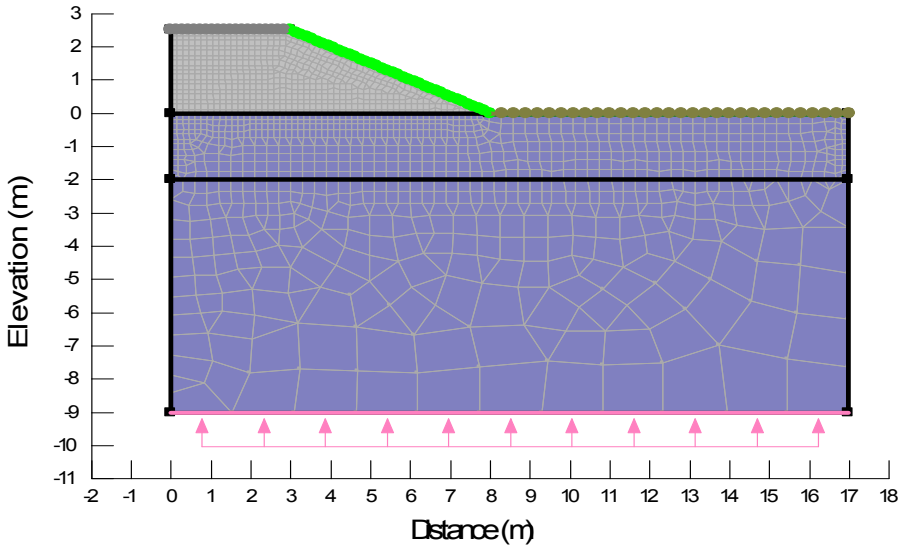

Figure 1. Finite element domain.

Figure 2 shows the analysis tree (KeyIn | Analyses). A steady-state SEEP/W-AIR/W and TEMP/W analysis are required to establish the initial pore-water/pore-air and temperature conditions, respectively. The steady-state analyses serve as the initial condition for the transient analyses, which is indicated by the relative position in the Analysis Tree. The addition of a transient convective heat transfer analysis adds both a transient SEEP/W-AIR/W analysis and the corresponding TEMP/W analysis. The analyses are solved simultaneously in a to-and-fro manner. TEMP/W uses the liquid water and air fluxes to compute and assemble the advective heat (energy) transfer terms into the global finite element equations. Incidentally, the hydraulic boundary conditions discussed subsequently are defined to create hydrostatic water and therefore no heat advection with the liquid water phase.

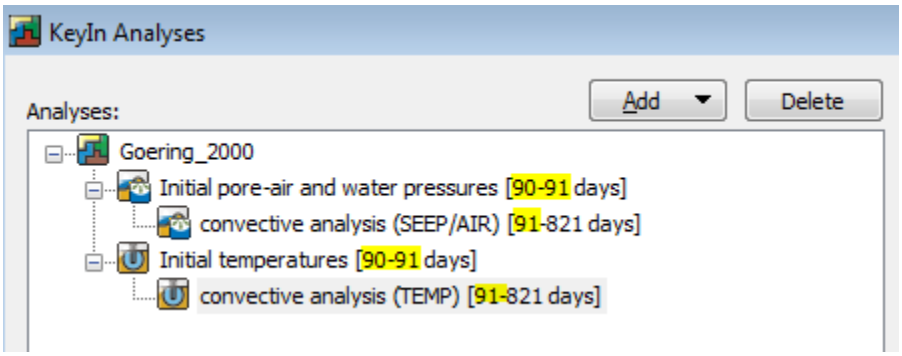

Figure 2. Analyses tree.

3.1 Material Properties

Consideration must be given to both the hydraulic (water and air) and thermal properties of the embankment and foundation soils. Both the foundation soil and embankment need to be simulated using the Saturated/Unsaturated material model because of the requirement for an air conductivity function. The foundation soil is silt with high moisture content; therefore, a negligible air hydraulic conductivity of 0.001 m/day was assumed. A non-zero value for air conductivity is required even if the soil is saturated so that the finite element equations can be solved. The arbitrary value should not be unnecessarily small to prevent numerical ill-conditioning of the global finite element matrices.

Goering (2000) reports an intrinsic permeability k for the for granular embankment material of 6.3E-7 m^2. The intrinsic permeability of a fluid is related to the hydraulic conductivity K by:

$$k = \frac{K\mu}{\gamma}$$

where μ is dynamic viscosity and γ unit weight. Assuming $\mu = 1.78E-05\ kg/(m-s)$ and $\gamma = 11.81\ N/m^3$ results in an air hydraulic conductivity of about 36,000 m/day. The air fluxes are used to compute and assemble the advective heat (energy) transfer terms into the global finite element equations. Extremely large air fluxes, created by the use of extraordinarily high air conductivity, can also create ill-conditioned global finite element matrices, resulting in premature termination of the solvers.

Goering (2000) noted that the ground surface cooling must be significant and the air conductivity sufficiently large for natural convection of the pore-air to occur during the winter months. The analysis was solved using air conductivities for the porous embankment of 10, 100, 1,000 and 10,000 m/day. Only the later resulted in the development of multiple convective cells that altered the conduction temperature isotherms. Although this value was less than 36,000 m/day, the resulting air flux rates provided for a numerically stable analysis while producing convective cells. Lastly, it is worth noting that Goering (2000) did not indicate a value of air hydraulic conductivity. The only value supplied in the paper was the intrinsic permeability.

The primary objective of the analysis was to simulate air and convective heat transfer within the porous embankment resting on a saturated foundation soil. The embankment material is essentially dry and the water within the foundation is assumed static. As such, the hydraulic properties are arbitrary. A negligible – but not unreasonable – hydraulic conductivity was assigned to both the embankment material and silt foundation soil. The volumetric water content functions are also arbitrary because there is no storage or release of water during the transient simulation. In addition, the volumetric water content functions are not used by Simplified Thermal and Full Thermal material models discussed subsequently. The arbitrary functions were estimated from the sample functions Gravel for the embankment and Silt for the foundation soil.

Figure 3 shows the thermal properties used for the embankment and silt foundation (Goering, 2000). Thermal conductivity and volumetric heat capacity is specified for both the frozen and unfrozen states. The Simplified Thermal and Full Thermal material models were used to represent the porous embankment and silt foundation, respectively. The sample thermal functions for Silt were used to create the thermal conductivity and unfrozen volumetric water content functions used by the Full Thermal material model. Both models require specification of volumetric water content in order to calculate the latent energy storage or release during freezing or thawing events. A negligible value of 0.01 was used to represent the dry embankment. Goering (2000) reports a moisture content of 0.45 for the silt foundation and dry density of 1442 kg/m^3. Goering (2000) did not specify if the moisture content was mass or volume based. Assuming the stated moisture content was mass based gives a void ratio of 0.55 assuming specific gravity of 2.7. The volumetric water content is calculated as 0.36 from the void ratio and is equal to the porosity.

Porous Embankment (Simplified Thermal Model)		
thermal K (frozen)	30	kJ/day/m/C
thermal K (unfrozen)	30	kJ/day/m/C
vol. heat capacity (frozen)	1020	kJ/m3/C
vol. heat capacity (unfrozen)	1020	kJ/m3/C
volumetric water content	0.01	
Silt Foundation (Full Thermal Model)		
thermal K (frozen)	186	kJ/day/m/C
thermal K (unfrozen)	173	kJ/day/m/C
vol. heat capacity (frozen)	1640	kJ/m3/C
vol. heat capacity (unfrozen)	2010	kJ/m3/C
volumetric water content	0.36	

Figure 3. Thermal properties for the embankment and foundation soils.

The latent heat of fusion for water is an important parameter in a heat flow analysis involving ground freezing (Set | Units and Scale). The default value in TEMP is 334,000 kJ/m^3, which is representative of pure water. Goering (2000) specified a value of only 26,200 kJ/m^3. The inclusion of latent heat effects in a heat transfer analysis produces a highly non-linear problem that requires special algorithms to prevent numerical oscillation (i.e. non-convergence). The reduction of the latent heat coefficient by over an order of magnitude would certainly promote convergence while altering the propagation of the freezing and thawing front in the foundation soil. The default value provided by TEMP was retained, which would naturally lead to some difference in the solution as compared to Goering (2000).

3.2 Boundary Conditions

Steady-State Analyses (Initial Conditions)

The steady-state SEEP/W-AIR/W analysis was completed by applying a hydraulic water head of 0 m to the line representing the original ground surface. A pore-air pressure of 0 kPa was applied to the top of the embankment. The boundary conditions result in hydrostatic pore-air and pore-water distributions. Alternatively, a pore-water pressure boundary condition could be applied to the regions comprising the embankment and foundation; however, this results in a hydraulic pore-water head gradient. An unreasonably low water hydraulic conductivity is then required to restrict flow during the transient analysis.

The steady-state TEMP/W analysis was completed by applying a temperature of -2 C to the entire domain.

Transient Convective Heat Flow Analyses

A total head of 0 m was applied to the entire domain throughout the duration of the SEEP/W transient analysis. This boundary condition ensures that the water remains hydrostatic, despite the fluctuation in air pressure (which produces a tendency for changes in water storage).

The top of the embankment was simulated using a no-flow air boundary (i.e. no air boundary condition applied) to represent the negligible air hydraulic conductivity of asphalt. Goering (2000) simulated the side-slope using both a no-flow boundary condition and an air pressure boundary condition that obeyed a harmonic function. In this study, all sides of the domain were assumed impermeable and therefore

modeled as a no flow (air) boundary condition. As noted above, this condition represents coverage by high moisture content topsoil or snow cover during the winter months.

Goering (2000) used the N-factor approach to determine harmonic temperature functions that were representative of the temperature on the asphalt surface, side-slope, and native soil surface. The function was given by:

$$T = A - Bcos\left(\frac{2\pi(t-9)}{365}\right)$$

where t is the Julian Day Number, A yearly mean temperature, and B the amplitude of the harmonic function. The coefficient A was set equal to 1.1, 2.7, and -1.9 C for the asphalt, side-slope, and native soil respectively. The coefficient B was set equal to 26.1, 20.9, and 10 C for the asphalt, side-slope, and native soil respectively. Figure 4 shows the harmonic temperature functions along all three surfaces (KeyIn | Thermal Boundary Functions). The functions were defined over 365 days and the option to cycle (the function) was selected. Goering (2000) notes that the mean temperature of the native soil of -1.9 C promotes permafrost while the mean temperatures of the embankment surfaces are above 0 C and therefore promote deterioration of the permafrost.

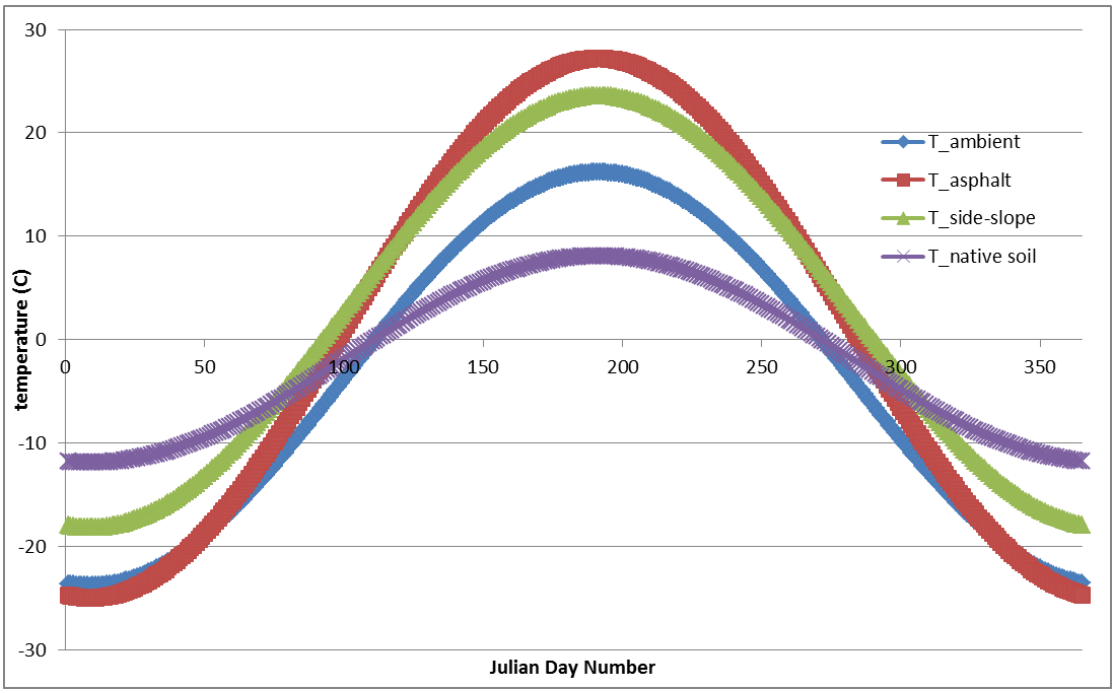

Figure 4. Harmonic temperature fluctuation with time given by Julian Day Number.

The left (symmetry) and right boundaries were considered adiabatic in the TEMP/W analysis. A geothermal ground heat flux of 5.2 kJ/day/m^2 (0.06 W/m^2) was applied to the bottom of the domain.

3.3 Time Steps

Goering (2000) simulated the harmonic temperature distribution cycling for 25 years using time steps of 0.25 days. The purpose of the long simulation time was to obtain the periodic annual cycles of air flow and heat transfers that govern the conditions of the foundation soil. Goering (2000) presented results for the last year of the simulation on August 1 and February 1, which are the periods during the cycle at which conduction and convection dominate the heat transfer, respectively.

For demonstrative purposes, the convective heat flow analysis was only solved for two cycles of the thermal boundary functions. The duration of the convective analysis was therefore specified as 730 days (KeyIn | Analyses). The Julian Day Numbers for August 1 and February 1 dates on the 1st and 2nd cycle of the simulation are 214/579 and 397/762, respectively. These specific elapsed times were entered into the list that appears at the bottom of the Time tab (KeyIn | Analyses), making data available on these days for graphing and contouring.

The transient analysis needed to be initiated at a time that provided boundary temperatures that were similar to the initial ground temperature of -2 C. The temperatures of the boundary functions on March 31 (Julian Day # 91) ranged between about -1 C and -3.5 C (Figure 4); consequently, Day 91 was selected to initiate the transient analysis. This was facilitated by specifying a starting time of 90 days and duration of 1 day in the steady-state analysis (Figure 2), which forces the start time of the Child Analysis to be Day 91.

The transient analysis was completed using 1 day steps with adaptive time stepping. Adaptive time stepping was used to promote convergence during the freeze/thaw cycles even though it may be possible to complete the entire analysis using 1 day time steps. A minimum and maximum allowable time step of 0.25 day and 1.0 day, respectively, were specified in the adaptive stepping settings.

4 Results and Discussion

Goering (2000) provides an insightful discussion on the physical process operating to promote convective cooling. Only a brief summary of some of the highly relevant results are provided. As will be apparent, the results of the simulations are comparable despite some important difference between the simulations, including:

1. An order of magnitude difference in the latent heat of fusion for the foundation soil;
2. Potential discrepancies in the air hydraulic conductivity of the porous embankment (i.e. the corresponding air conductivity used by Goering (2000) is unknown);
3. Differences in time stepping strategies;
4. Differences in the physics (partial differential equations), element types (meshing), and integration order;
5. Difference in the finite element formulations and solution strategies (e.g. the water transfer equations are being solved simultaneously with the air and heat transfer equations while Goering (2000) solved only the air and heat transfer equations);
6. Differences in the algorithms required to handle latent heat effects; and,
7. Goering (2000) simulated 25 cycles, while only 2 cycles were simulated using the TEMP/W convective heat transfer analysis.

Figure 5 compares the simulated convective cells on February 1 of the 2nd cycle (Julian Day # 762). Two large and dominate convective cells develop below the pavement surface, circulating the air in clockwise (centerline) and counterclockwise directions. Three convective cells develop beneath the side-slope. Goering (2000) calculated a mean velocity of 8.8 m/hr (Figure 5). A mean velocity of about 6 m/hour was produced by the GeoStudio simulation. The average was calculated in a spreadsheet after using (Draw | Graph) to obtain the air xy-velocities for all nodes within the region comprising the embankment.

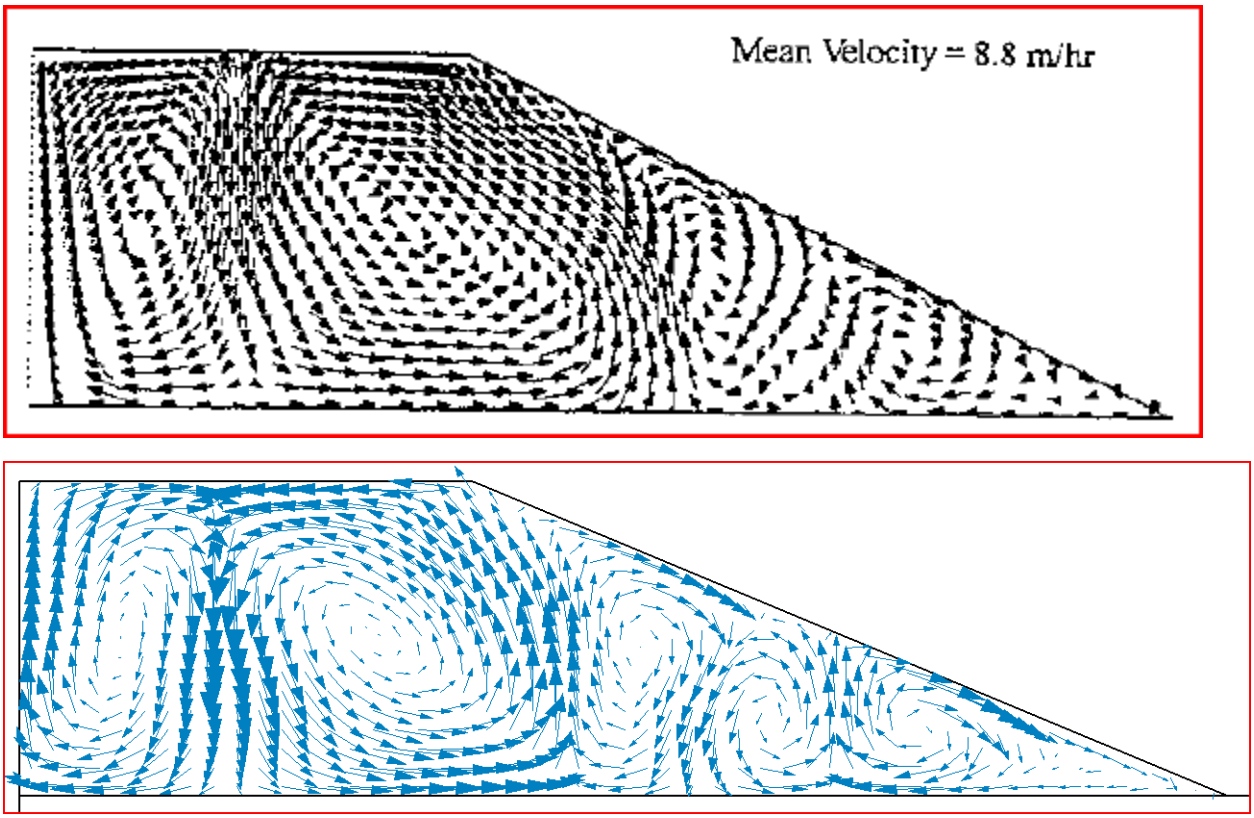

Figure 5. AIR/W pore-air flux vectors (bottom) on February 1 of the 2nd cycle (Julian Day # 762) as compared to Goering (2000).

Goering (2000) notes that a critical temperature difference between the upper and lower boundaries must be exceeded for natural convective cells to develop. Convection occurs during the portion of the climate (temperature) cycle when there is a relatively low temperature at the surface compared to the warmer temperature near the base of the embankment. Figure 6 shows the temperature history at a node at the interface between the embankment and foundation as compared to the harmonic temperature function applied to the pavement surface. The convective air cells initiate circulation as early as about Julian Day Number 321 and 681 on the 1st and 2nd cycles when the base of the embankment is around 0 C. The asphalt surface had not yet reached its coldest point when the critical temperature difference was exceeded.

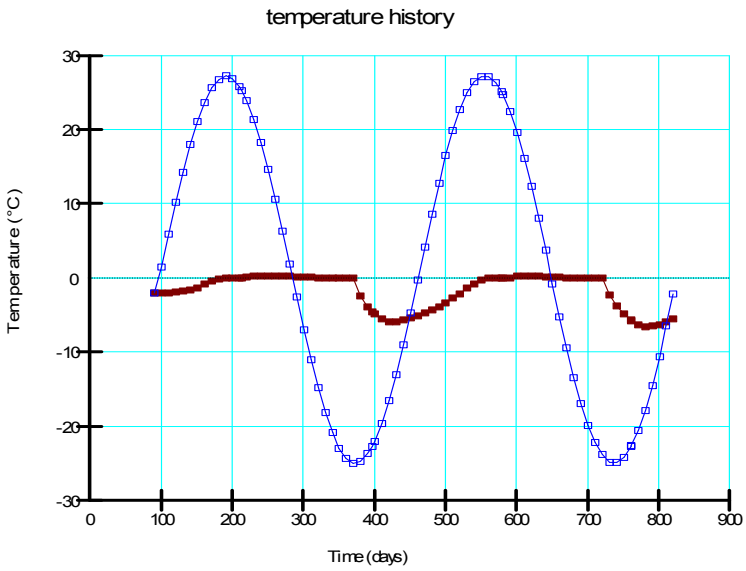

Figure 6. Temperature history at the interface between the embankment and foundation along the line of symmetry as compared to the harmonic asphalt temperature.

Figure 7 shows the temperature plume structures that develop due the large air flux rates within the convective cells. The pattern of temperature contours matches the pore-air convective cells. The cells form during the winter months due to the unstable pore-air density stratification within the embankment (Goering, 2000). The plume beneath the driving lane simulated by GeoStudio in the 2nd cycle compares well with Goering (2000) after the 25th cycle as is evidenced by the -16 C and -14 C contours. The -4 C contour is also at a nearly identical location within the foundation soil. Goering (2000) notes that the influence of the plume is evidenced by the fact that the -4 C contour has penetrated almost as deep beneath the centerline as it has beneath the native land surface, despite the 2.5 m of coarse overburden.

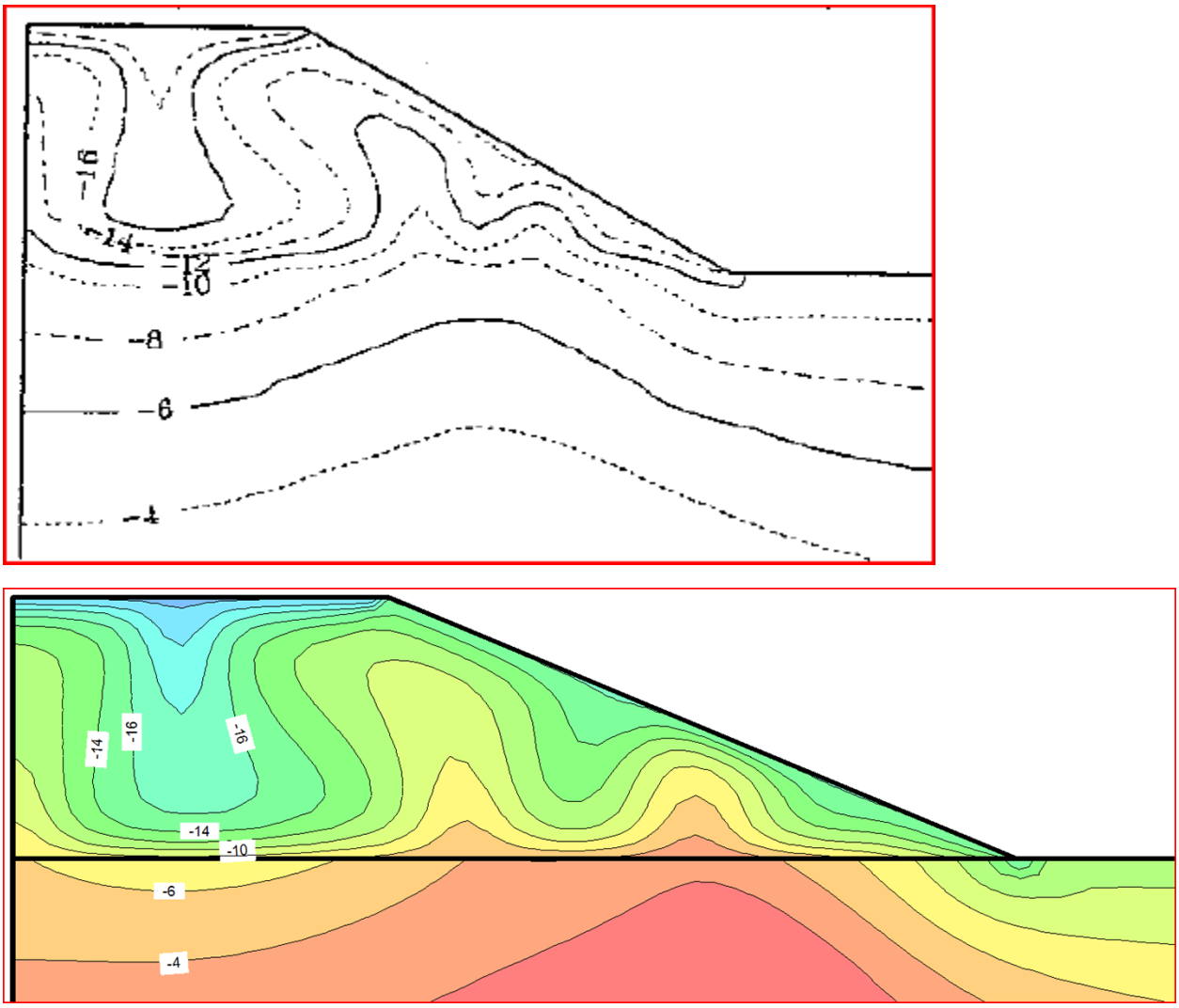

Figure 7. AIR/W temperature contours (bottom) on February 1 of the 2nd cycle (Julian Day # 762) as compared to Goering (2000).

During the summer months, the pore-air density gradient is more stable and the air fluxes are negligible. Conduction dominates the heat transfer process and temperature contours are relatively horizontal within the embankment (Figure 8). Goering (2000) notes that the depth of thaw has not progressed as deep into the foundation soil beneath the embankment than it has beneath the native land surface.

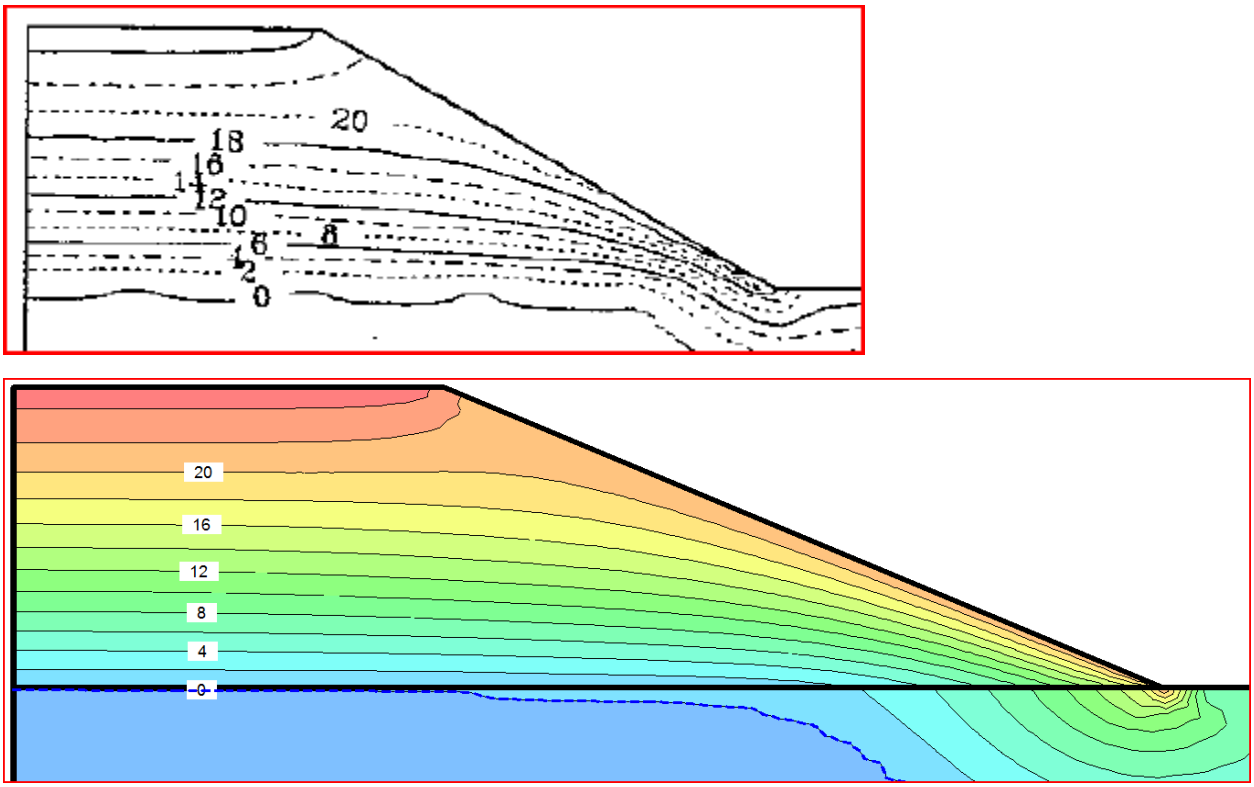

Figure 8. AIR/W temperature contours (bottom) on August 1 of the 2nd cycle (Julian Day # 579) as compared to Goering (2000).

Figure 9 shows the measured temperatures within the test embankment on August 1 and February 1. The external conditions imposed on the embankment deviated considerably from those simulated. Despite these variations, the numerical simulations reproduce the temperature patterns and help elucidate the mechanisms controlling the potential for thaw of the permafrost. The measured temperatures clearly reflect the existence of convective activity within the embankment during the winter months and conduction dominant heat transfer during the summer months (Goering, 2000).

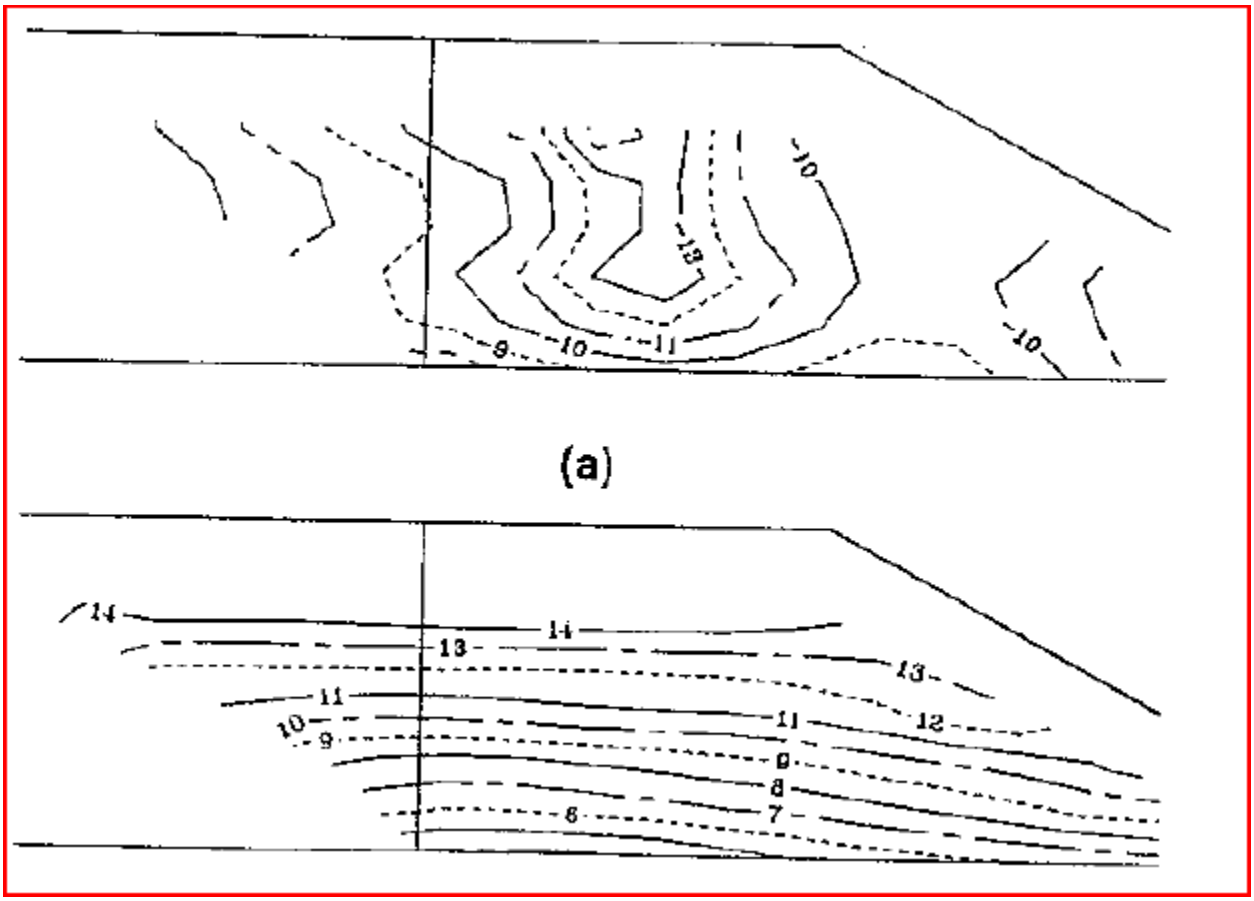

Figure 9. Measured temperature contours on February 1 and August 1 (Goering, 2000)

5 Summary and Conclusions

SEEP/W and AIR/W can be used in combination with TEMP/W to simulate passive cooling within coarse materials due to the development of convective cells. Passive cooling can prevent thaw of underlying permafrost, thus eliminating thaw settlement (Goering, 2000). Goering (2000) also notes that natural convection in coarse material can cause enhanced seasonal freezing beneath embankments and therefore exacerbate problems with frost heave in foundation soils for certain climates. That is to say, passive cooling is only advantageous in some (cold) climates.

6 References

Goering, D.J. and Kumar, P. 1996. Winter-time convection in open-graded embankments. Cold Regions Science and Technology, 24, 57-74.

Goering, D.J., 1998. Experimental investigation of air convection embankments for permafrost-resistant roadway design. Proceedings of the 7th International Conference on Permafrost, Yellowknife, NWT, 319-326.

Goering, D.J. 2000. Passive cooling of permafrost foundation soils using porous embankment structures. American Society of Mechanical Engineers (ASME), Heat transfer Division, 366-5, 103-111.